The comparison of the analytical contact conductance model[7,8] to describe $R_{jb}$ and the experimentally obtained values is shown in Table 3. Uncertainty in the parameters used in the analytical model was estimated to be 3.5%, and the error associated with the experimental values was computed using a 95% confidence interval. However, it is not uncommon for hardness to vary ±10% for essentially homogeneous materials such as aluminum. Hardness of heterogeneous materials, such as carbon composite, may vary greatly, depending upon the number and depth of fibers below the surface.

The summary presented in Table 3 shows a considerable decrease in the composite contact resistance to that of aluminum. This could be attributed to aluminum oxide that could have formed. Although not confirmed, the decrease in contact resistance with the composite could be attributed to composite fibers coming in contact with the die surface, allowing for more conduction paths.

## Conclusions

Experiments were performed to investigate the effects of contact and spreading resistance as applied to the cooling of an OLGA package. There were two types of heat sinking materials used, aluminum and carbon composite. The composite material proved to have higher overall performance, as measured by the lower overall junction-to-ambient thermal resistance. Closed-form analytical expressions characterizing contact resistance and spreading resistance were shown to be accurate in predicting both heat transfer processes, even though the analytical models were not calibrated using composite material.

Heat transfer across an interface is complex because the thermal resistance can depend on many geometric, thermal, and mechanical parameters. Separating the overall thermal resistance into constituent components allows for comparison of the contributions. The experiments presented here show that the interface contact resistance can account for as much as 50% of the total thermal resistance. The results presented here imply that we cannot ignore the effects of contact resistance in the application of electronic cooling. As die and packages continue to decrease in size, and power dissipation continues to increase, the contact resistance and thermal spreading processes will only be exacerbated.

## References

[1]"Part 1 Measurement Uncertainty—Instruments and Apparatus," ANSI/ASME PTC 19.1-1985, American Society of Mechanical Engineers, New York, 1986.

[2]Song, S., Lee, S., and Au, V., "Closed-Form Equation for Thermal Constriction/Spreading Resistances with Variable Resistance Boundary Condition," *Proceedings of the 1994 International Electronics Packaging Conference* (Atlanta GA), 1994, pp. 111–121.

[3]Fletcher, L. S., "Recent Developments in Contact Conductance Heat Transfer," *Journal of Heat Transfer*, Vol. 110, 1988, pp. 1059–1070.

[4]Lambert, M. A., and Fletcher, L. S., "Review of the Thermal Contact Conductance of Junctions with Metallic Coatings and Films," *Journal of Thermophysics and Heat Transfer*, Vol. 7, No. 4, 1993, pp. 547–554.

[5]Madhusudana, C. V., and Fletcher, L. S., "Contact Heat Transfer—The Last Decade," *AIAA Journal*, Vol. 24, No. 3, 1985, pp. 510–523.

[6]Yovanovich, M. M., and Antonetti, V. W., "Application of Thermal Contact Resistance Theory to Electronic Packages," *Advances in Thermal Modeling of Electronic Components and Systems*, edited by A. Bar-Cohen and A. D. Kraus, Vol. 1, 1988, pp. 79–128.

[7]Antonetti, V. W., Whittle, T. D., and Simons, R. E., "An Approximate Thermal Contact Conductance Correlation," *Journal of Electronic Packaging*, Vol. 115, 1993, pp. 131–134.

[8]Madhusudana, C. V., *Thermal Contact Conductance*, Springer–Verlag, New York, 1996, pp. 1–61.

# Experimental and Numerical Study of Thermovibrational Convection

R. Monti,* R. Savino,† and G. Alterio‡
*University of Naples, Piazzale Tecchio 80-80125, Naples, Italy*
and
R. Fortezza§
*Microgravity Advanced Research and Support Center, Via Comunale Tavernola, 80144 Naples, Italy*

## Nomenclature

$b$ = displacement, cm
$f$ = frequency, Hz
$g_0$ = acceleration of gravity, 981 cm/s$^2$
$H$ = vertical length (along $y$ axis), cm
$L$ = horizontal length (along $x$ axis), cm
$Pr$ = Prandtl number, $\nu/\alpha$
$Ra_g$ = gravitational Rayleigh number, $g\beta_T\Delta TL^3/\nu\alpha$
$Ra_v$ = vibrational Rayleigh number, $(b\omega\beta_T\Delta TL)^2/2\nu\alpha$
$T$ = temperature, K
$\alpha$ = thermal diffusivity, cm$^2$/s
$\beta_T$ = thermal expansion coefficient, K$^{-1}$
$\Delta T$ = temperature difference, K
$\mu$ = dynamic viscosity, g cm$^{-1}$ s$^{-1}$
$\nu$ = kinematic viscosity, cm$^2$/s
$\rho$ = fluid density, g/cm$^3$
$\omega$ = angular frequency, s$^{-1}$

## Introduction

THE phenomenon of thermovibrational convection has been extensively investigated in Russian literature.[1–3] In the pioneering theoretical studies of Gershuni and Zhukhovitskii,[1] the influence of high-frequency vibrations on the behavior of liquids, in the presence of a thermal gradient, was studied by time-averaging the fluid dynamic equations. One of the most important results of these studies was that vibrations of a fluid cell, in the presence of temperature gradients, may induce a convective flow that, in turn, distorts the temperature distribution, compared with the purely diffusive situation. The experimental results obtained by Zavarykin et al.[2,3] confirmed the existence of thermovibrational convection in a liquid vibrating in the presence of a temperature gradient in Earth's gravity field.

The present authors point out that these effects may be particularly important during fluid and material science microgravity experimentation on the International Space Station,[4] where the residual gravity is reduced by several orders of magnitude and high-frequency $g$-jitter may be sources of acceleration disturbances. The study of thermovibrational effects on fluid and material science experiments is of primary importance, for the appropriate planning of the space activities and for the postflight analysis of the results obtained.

Recent theoretical and numerical studies in this field[5,6] have shown that, in the range of frequencies of interest for the space

Received Jan. 26, 1998; revision received Aug. 3, 1998; accepted for publication Aug. 6, 1998. 

*Professor of Aerodynamics, Dipartimento di Scienza e Ingegneria dello Spazio "Luigi G. Napolitano." E-mail: monti@unina.it. Member AIAA.

†Researcher, Dipartimento di Scienza e Ingegneria dello Spazio "Luigi G. Napolitano." E-mail: rasavino@unina.it.

‡Ph.D. Student, Dipartimento di Scienza e Ingegneria dello Spazio "Luigi G. Napolitano."

§Researcher. E-mail: fortezza@mars.unina.it.

station ($10^{-6} \leq g/g_0 \leq 10^{-2}$; $10^{-1}$ Hz $\leq f \leq 10^2$ Hz), the oscillatory parts of the temperature and/or concentration distortions are negligible when compared with their time-averaged counterparts, induced by the time-averaged velocity field. This is particularly true in high Prandtl number liquids, for temperature distortions, or in doped systems with large Schmidt numbers, for concentration distortions, with very long characteristic diffusion times.

To confirm the numerical results, a microgravity experiment is under definition. To prepare the flight experiment, a number of experimental and numerical research activities on the ground are in progress. In particular, preliminary experimental measurements have been performed using an infrared thermocamera to detect the temperature distribution in different vibration conditions, and three-dimensional numerical simulations have been carried out to correlate the experimental results.

## Experimental Facility and Numerical Model

To prepare the flight experiment, a prototype of the test cell has been developed. The main component of the facility is a Plexiglas® cubic cell whose side is 5 cm. Two opposite copper plates can be maintained at different temperatures. The cell is mounted on a sled that can vibrate in one direction, with sinusoidal oscillations of prescribed frequencies and amplitudes (0.1 cm $\leq b \leq$ 2 cm; 1 Hz $\leq f \leq$ 15 Hz). The accelerations are measured by an accelerometer. The flowfield in the liquid can be visualized by tracer particles. The surface temperature distribution is measured by an AGEMA thermocamera operating in the long-wave infrared band (8–12 $\mu$m).

The numerical simulations are based on the solution of the time-dependent, three-dimensional Navier–Stokes equations, using a finite difference technique in a staggered grid. The field equations are solved explicitly in time using a modified marker and cell (MAC) method.[7]

## Results and Discussion

To validate the code, a case study has been performed dealing with the Rayleigh instability of a liquid in the cell heated from below.[8] The comparison between the experimental and numerical streamlines in the midsection of the cavity, and between the numerical and experimental surface temperature distribution at the lateral wall, measured with the thermocamera, revealed a sufficient agreement between experimental and numerical results. To investigate the influence of vibrational effects, purely diffusive conditions were first established, cooling

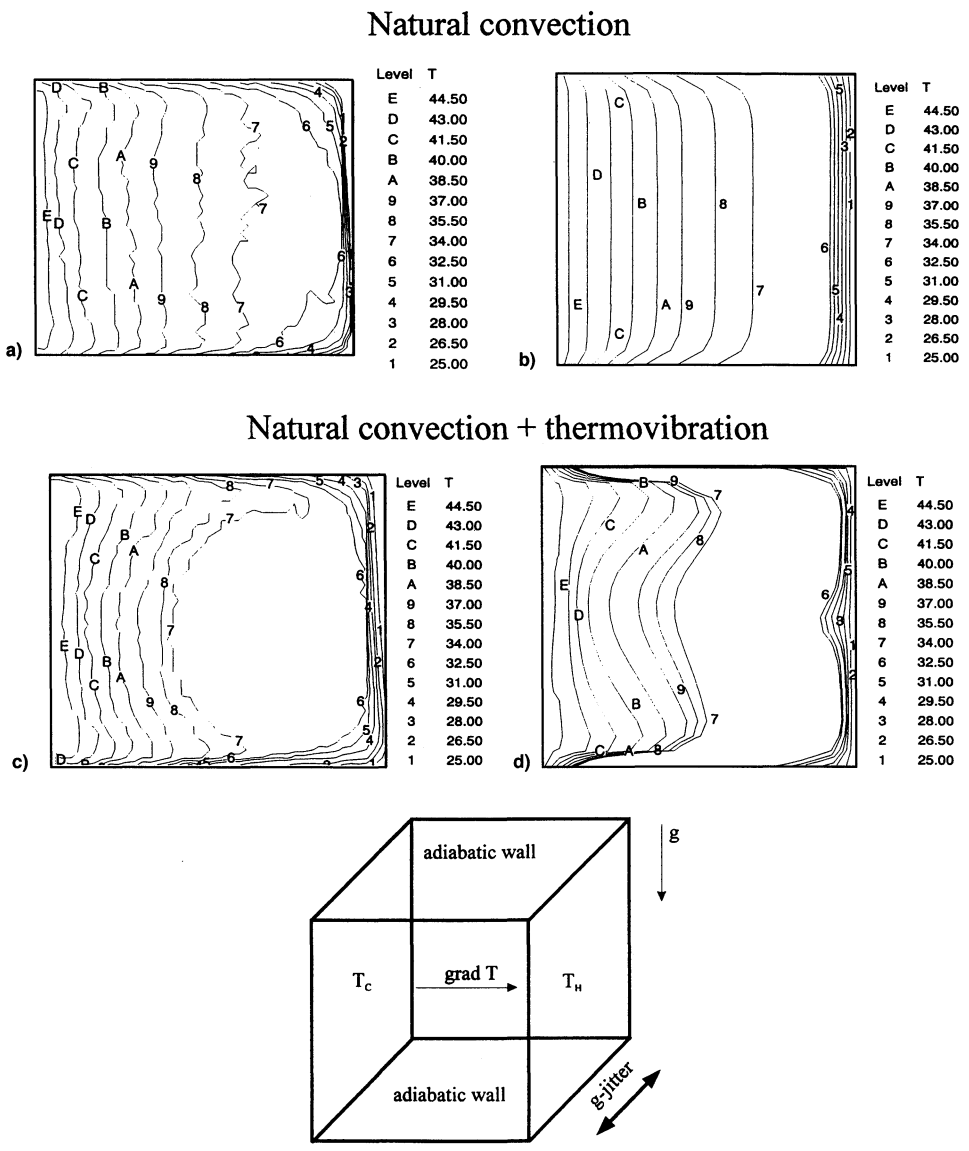


**Fig. 1 Surface temperature distribution on the horizontal top wall of the cell. The vertical walls are maintained at different temperatures, $\Delta T$ = 20 K: a) natural convection only, experimental; b) natural convection only, numerical; c) natural convection plus sinusoidal vibrations ($b$ = 2 cm, $f$ = 7 Hz), experimental; and d) natural convection plus sinusoidal vibrations ($b$ = 2 cm, $f$ = 7 Hz), numerical. The liquid is silicone oil 3 cS.**

the bottom plate and heating the upper one, i.e., imposing a vertical temperature gradient opposite the direction of the gravity vector, by establishing a temperature difference of $\Delta T$ = 30 K.

At this point, sinusoidal oscillations ($b$ = 1 cm, $f$ = 10 Hz) were applied in the direction orthogonal to the thermal gradient. This is the same configuration investigated theoretically by Gershuni et al.,[9] assuming two-dimensional flow and zero gravity. In the present case ($g = g_0$), no temperature distortions were detected by the thermocamera images and no tracers motion by the video camera. This result, in agreement with the numerical calculations, shows that for this configuration, thermovibrational effects are negligible because of the stabilizing gravitational effects on Earth. This is not in contradiction with the experimental results of Zavarykin et al.,[3] who found that vibrations normal to the temperature gradient in a stable stratified liquid can induce flow in the system. In fact, Zavarykin et al.[3] considered a thin horizontal convection chamber (with eight $H$ ranging from 1 to 5 mm) and much larger vibrations ($b$ = 4 cm, $f$ = 25 Hz); in this layer the relative importance between vibrational and stabilizing buoyancy effects is much larger.

In the second configuration investigated, the test cell was fixed vertically on the sled and the temperature gradient was applied in the horizontal direction, i.e., orthogonal to the direction of the gravity vector. Figures 1a and 1b show the measured and computed surface temperature distributions for the steady conditions, in the case of natural convection only ($\Delta T$ = 20 K). The structure of the isotherms shows the presence of a main vortex cell in the vertical section, where the liquid rises along the hot wall and flows down along the cold one.

At this time, horizontal vibrations were applied (in the direction orthogonal to the gravity vector and to the temperature gradient). The sinusoidal oscillations were characterized by $b$ = 2 cm, $f$ = 7 Hz ($Ra_v = 5.4 \times 10^6$). Figures 1c and 1d show that, in these conditions, an asymmetrical temperature distribution appears, demonstrating that an averaged convective motion in this plane exists.

## Thermovibrational Convection in a Fluid Cell with Large Aspect Ratio

Comparing the gravitational and vibrational Rayleigh numbers, defined by

$$Ra_g = \frac{g_0 \beta_T \Delta T H^3}{\nu\alpha}, \qquad Ra_v = \frac{(b\omega\beta_T \Delta T L)^2}{2\nu\alpha} \tag{1}$$

it is evident that the relative importance between thermovibrational and residual-gravity ($g_0$) effects is represented by the nondimensional ratio

$$\frac{Ra_v}{Ra_g} = \frac{b^2\omega^2\beta_T \Delta T}{2g_0 H}\left(\frac{L}{H}\right)^2 \tag{2}$$

To enhance the relative thermovibration effect one should adopt 1) liquids with a particularly large thermal expansion coefficient ($\beta_T$), 2) relatively large vibrations velocity ($b\omega$), 3) a geometrical configuration with large aspect ratio ($L/H$), and 4) small height ($H$).

For this purpose, a test cell with a vertical dimension ($H$) of only 3 mm was employed. Zavarykin et al.[2,3] considered a similar configuration; however, in their study, the two rectangular plates (vertical or horizontal) were maintained at different temperatures, i.e., the imposed temperature gradient was in the direction of the liquid-layer thickness and the vibrations in the plane of the isothermal plates. On the contrary, to obtain adequate infrared thermocamera images, the temperature gradient, in the present configuration, is directed from the left side (maintained at a higher temperature) to the right side (maintained at a lower temperature), i.e., the temperature gradient is horizontal.

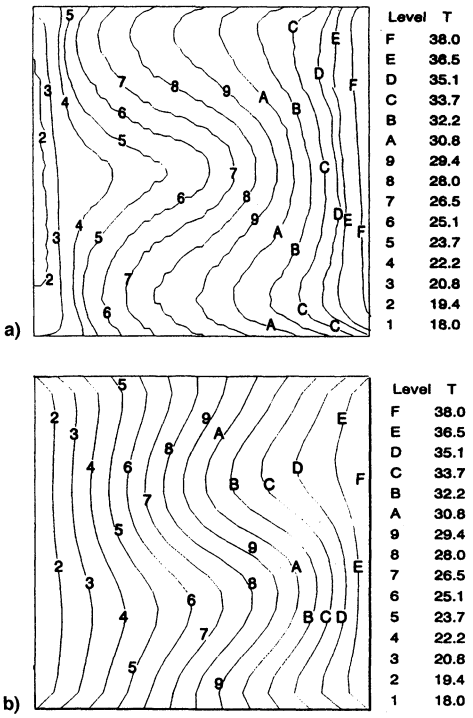


**Fig. 2 Surface temperature distribution on the horizontal top wall of the test cell with large aspect ratio. The left and right vertical walls are maintained at different temperatures, $\Delta T$ = 20 K. Sinusoidal vibrations ($b$ = 2 cm, $f$ = 9 Hz) are applied in the horizontal plane, normal to the temperature gradient: a) experimental and b) numerical. The liquid is water.**

To minimize the effects of natural convection, the test cell has been leveled by using micrometric adjustment. This is necessary because a small inclination angle ($\gamma$), with respect to the local vertical direction, is responsible for an asymmetric surface temperature distribution caused by buoyancy convection. For $\gamma$ = 0, in the absence of vibrations, buoyancy convection is minimized and the temperature distribution is almost coincident with the diffusive one. Starting from this condition, sinusoidal oscillations have been applied in the direction orthogonal to the thermal gradient and to the gravity vector.

Figure 2 shows the experimental and numerical surface temperature distributions at the periodic state, for $\Delta T$ = 20 K, and a vibration characterized by $b$ = 2 cm, $f$ = 9 Hz. The liquid employed is distilled water. The results indicate that, increasing the vibrations, thermovibrational effects give rise to relevant distortions of the temperature field (in the absence of vibrations the upper surface distribution is similar to that of Fig. 1b). Similar behavior occurs for prescribed vibrations if the temperature difference is increased.

It must be pointed out that the amplitudes of the vibrations considered in the present work are much larger, compared with those considered in previous numerical simulations dealing with microgravity fluid science experiments that are only marginally affected by oscillatory disturbances.[10] In fact, as explained in the Introduction, the objective of this work was the preparation of a microgravity experiment to confirm previous numerical results on the role and on the physical mechanisms associated with thermovibrational effects, particularly in the presence of rare events, e.g., strong oscillatory disturbances induced, e.g, by crew activities, ergometer, etc. For this reason, larger disturbance amplitudes have been considered.

## Conclusions

According to the numerical results, the experiments pointed out that to study thermovibrational convection on the ground, where the Earth gravity field masks the vibration effects, it is necessary to increase the geometrical aspect ratio $L/H$. Exper-

iments performed in a test cell with aspect ratio $L/H = 16$ have shown that steady thermal distortions arise in the presence of relatively large $g$-jitter at relatively high frequencies. These distortions depend on the value of the vibrational Rayleigh number (proportional to the temperature difference and to the velocity of the $g$-jitter oscillations).

An experimental proposal is being considered for the International Space Station, where the steady residual gravity is reduced by several orders of magnitude, compared with Earth conditions, so that a fluid cell with unitary aspect ratio could be used and relatively small $g$-jitter will be sufficient to induce measurable thermofluiddynamic distortions.

## References

[1]Gershuni, G. Z., and Zhukhovitskii, E. M., *Convective Stability of Incompressible Fluids*, Keterpress Enterprises, Jerusalem, Israel, 1976.

[2]Zavarykin, M. P., Zorin, S. V., and Putin, G. F., "Experimental Study of Vibrational Convection," *Fluid Mechanics—Translation of Soviet Physics Doklady*, Vol. 37, No. 4, 1985, pp. 267, 268.

[3]Zavarykin, M. P., Zorin, S. V., and Putin, G. F., "Convective Instabilities in a Vibrational Field," *Fluid Mechanics—Translation of Soviet Physics Doklady*, Vol. 33, No. 3, 1988, pp. 174–176.

[4]Monti, R., and Savino, R., "A New Approach to $g$-Level Tolerability for Fluid and Material Science Experiments," *Acta Astronautica*, Vol. 37, No. 4, 1994, pp. 313–331.

[5]Monti, R., and Savino, R., "The Basis and Recent Developments of Napolitano's Scaling and Order of Magnitude Analysis," *Microgravity Quarterly*, Vol. 5, No. 1, 1995, pp. 13–17.

[6]Monti, R., and Savino, R., "Microgravity Experiments Acceleration Tolerability on Space Orbiting Laboratories," *Journal of Spacecraft and Rockets*, Vol. 33, No. 5, 1996, pp. 707–716.

[7]Fletcher, C. A. J., *Computational Techniques for Fluid-Dynamics*," Springer–Verlag, Berlin, 1991.

[8]Monti, R., Savino, R., Alterio, G., and Fortezza, R., "Experimental Study of Thermovibrational Convection," AIAA Paper 98-0736, Jan. 1998.

[9]Gershuni, G. Z., Zhukhovitskii, E. M., and Yurkov, Y. S., "Vibrational Thermal Convection in a Rectangular Cavity," *Fluid Dynamics—Translation of Izvestiya Akademii Nauk SSSR, Mekhanika Zhidkosti i Gaza.*, Vol. 17, No. 4, 1982, pp. 565–569.

[10]Kondos, P. A., and Subramanian, R. S., "Buoyant Flow in a Two-Dimensional Cavity Due to a Sinusoidal Gravitational Field," *Microgravity Science and Technology*, Vol. 9, No. 3, 1996, pp. 143–151.

# Satellite Mesh Reflector Temperature Measured by Using Fine Thermocouples

Akihiro Miyasaka*
*NTT Wireless Systems Laboratories, 1-1 Hikarinooka Kanagawa, 239-0837, Japan*

## Nomenclature

$A_1$ = solar power absorption area, $m^2$
$A_2$ = heat radiation area, $m^2$
$c_2$ = Planck's constant, m K
$F$ = solar flux, $W/m^2$
$S$ = luminance temperature, K
$T$ = temperature, K
$T_m$ = mesh temperature, K
$T_s$ = boundary temperature, K
$\alpha$ = solar absorptivity
$\varepsilon$ = infrared emissivity
$\lambda_e$ = effective wavelength, m
$\sigma$ = Stefan–Boltzmann constant, $W\ m^{-2}\ K^{-4}$
$\tau$ = transmissivity

Received July 16, 1998; revision received Aug. 10, 1998; accepted for publication Aug. 10, 1998. 

*Senior Research Engineer, Satellite Communication Systems Laboratories. Member AIAA.

## Introduction

THE weight of large-aperture space antenna reflectors can be effectively reduced by using mesh as the reflector surface.[1] The mesh is made of gold-plated metal filaments, and the woven configuration is determined by the radio frequency. The mesh shape is controlled by a cable network, which consists of surface cables, back cables, and tie cables.[2] The antenna reflector itself consists of a mesh surface, a cable network, and truss structure.[3] In the case of solar energy incident on the mesh, the estimated mesh temperature exceeds 473 K (200°C), when it is calculated from the surface properties of gold. At this temperature, the stiffness of surface cables attached to the mesh surface can change or the cables can become fused, and as a result, cable quality is an important design factor. The thermal deformation of a reflector can be evaluated by considering the temperature of the cables and the truss pipes. However, the mesh temperature affects the temperature of the cables and truss pipes, and no studies have been done to determine the mesh temperature; therefore, the extent of the problem is not known. In a conventional method, the temperature measured by ordinary thermocouples attached to the mesh is influenced by the surface properties of the thermocouples. Because the diameter of a thermocouple is 10 times greater than that of a mesh filament, the radiative and conductive heat transfer between a thermocouple and filaments is substantial. Therefore, it is difficult to measure an accurate mesh temperature using ordinary thermocouples. Thus, the correct mesh temperature has not yet been experimentally obtained. In this Note, we report experimental mesh temperature measurements that were done using fine thermocouples with diameters nearly equal to those of the mesh filaments. The experimental results were obtained by irradiating pseudosolar radiation on the mesh in a space environment simulation chamber. In addition, we compared the temperature measured by radiation thermometers and ordinary thermocouples with the measuements done using the fine thermocouples.

## Experiment

### Mesh and Thermocouple Combination

The meshes we tested are shown in Fig. 1. The magnified photographs reveal two texture sizes of mesh with fine thermocouples attached. The meshes were fixed on a frame with 500 kg/m of tension. Both meshes were composed of gold-plated filaments $3.0 \times 10^{-5}$ m in diameter. The fine thermocouples were Chromel–Alumel-type thermocouples and measured $5.0 \times 10^{-5}$ m in diameter. We also measured the mesh temperature using ordinary thermocouples and radiation thermometers. The ordinary and thermocouples were sewn through the mesh. The mesh was irradiated in a vacuum chamber, and the mesh temperature was measured. The solar power was varied from 600 to 1400 $W/m^2$. The temperature of each mesh was determined from the average values measured by the two fine thermocouples.

### Measurement by Radiation Thermometers

When measuring the temperature with a radiation thermometer, the correct emissivity must be set to measure an accurate temperature. However, it is difficult to determine the mesh emissivity when the effects of porous or gathered fine filaments are included. The emissivity is different for polished or sand-blasted surface conditions. Moreover, ordinary radiation thermometers do not work for emissivities less than 0.1. Radiation thermometers measure the radiance of a body to determine its